Titanium Triamidotriamine Compounds: Syntheses, Structures and Redox Properties

Ana M. Martins,*[a] José R. Ascenso,*[a] Cristina G. de Azevedo,[a] Alberto R. Dias,[a] M. Teresa Duarte,[a] Humberto Ferreira,[a] M. João Ferreira,[a] Rui T. Henriques,[b] M. Amélia Lemos,[c] Li Li,[a] and João F. da Silva[a]

Keywords: Amide ligands / Cyclic voltammetry / N ligands / Titanium

The preparation of 1,4,7-{NH(2-C_6H_4F)$SiMe_2$}$_3$-1,4,7-triazacyclononane ($H_3N_{3\text{-}F}[9]N_3$) and 1,4,8-{N(H)Ph$SiMe_2$}$_3$-1,4,8-triazacycloundecane ($H_3N_3[11]N_3$), and their sodium derivatives $Na_3N_{3\text{-}F}[9]N_3(THF)_2$ and $Na_3N_3[11]N_3(THF)_2$, is described. The reaction of [$TiCl_3(THF)_3$] with $Na_3N_{3\text{-}F}[9]N_3(THF)_2$ and $Na_3N_3[11]N_3(THF)_2$ leads to [Ti{$N_{3\text{-}F}[9]N_3$}] and [Ti{$N_3[11]N_3$}]. The titanium complexes react readily with I_2 to give the Ti^{IV} derivatives [Ti{$N_{3\text{-}F}[9]N_3$}]I and [Ti{$N_3[11]N_3$}]I. All titanium compounds display distorted trigonal prismatic geometries where the metal is coordinated to the six nitrogen donors. Fluxional processes that convert the conformations of the five- and six-membered metallacycles and the Δ and Λ enantiomers of [Ti{$N_3[11]N_3$}]I have been identified in solution.

Introduction

The *N*-functionalization of azamacrocycles has been extensively explored as a method to design new ligand frameworks for metal cations. Several substituents and synthetic methodologies have been described and aspects such as structures, stabilities and physical properties have been broadly explored for many compounds. Despite the large number of transition-metal complexes of polyaza macrocyclic ligands bearing functionalized pendant arms reported in the literature,[1–3] the number of compounds displaying amide-tacn fragments as metal donors is much lower.[4–8] In this context we have reported the synthesis of a new six-donor triamidotriamine ligand precursor derived from tacn by introducing three $Si(Me)_2N(H)Ph$ pendant arms on the nitrogen atoms, and the preparation and characterisation of several triamide-tacn metal derivatives.[9,10] The ligand is hexacoordinate in all these complexes, irrespective of the size or oxidation state of the metals used (Ti, lanthanides, U). With the aim of modifying the donor properties of the original set and reduce the ligands' hapticity, with concomitant release of coordination positions at the metal centres, we introduced *ortho*-fluorine substituents in the phenyl rings and increased the macrocyclic framework and replaced tacn with triazacycloundecane (tacu). Although this goal has not been attained, we describe here the syntheses and characterisation of the new ligand precursors together with their sodium, Ti^{III} and Ti^{IV} derivatives. To the best of our knowledge, Ti-tacu complexes have not been reported before. Cyclic voltammetry results are also presented.

[a] Centro de Química Estrutural, Complexo Interdisciplinar, Instituto Superior Técnico,
Av. Rovisco Pais, 1, 1049-001 Lisboa, Portugal
E-mail: ana.martins@ist.utl.pt
[b] Instituto Superior Técnico,
Av. Rovisco Pais, 1, 1049-001 Lisboa, Portugal
[c] Centro de Engenharia Biológica e Química, Instituto Superior Técnico,
Av. Rovisco Pais, 1, 1049-001 Lisboa, Portugal

Results and Discussion

The reaction sequence used to synthesize 1,4,7-[{N(H)-2-C_6H_4F}$SiMe_2$]$_3$-triazacyclononane (**1**, $H_3N_{3\text{-}F}[9]N_3$), 1,4,8-{N(H)Ph$SiMe_2$}$_3$-triazacycloundecane (**2**, $H_3N_3[11]N_3$) and their sodium derivatives $Na_3N_{3\text{-}F}[9]N_3(THF)_2$ (**3**) and $Na_3N_3[11]N_3(THF)_2$ (**4**) is presented in Scheme 1. $H_3N_{3\text{-}F}[9]N_3$ (**1**) and $H_3N_3[11]N_3$ (**2**) were obtained in quantitative yields from the corresponding triazamacrocycle trihydrochloride derivatives.[11,12] $Na_3(THF)_2N_{3\text{-}F}[9]N_3$ (**3**) and $Na_3(THF)_2N_3[11]N_3$ (**4**) were also isolated in quantitative yields from THF from the reaction of **1** and **2** with NaH, respectively.

The characterization data of **1**–**4** are consistent with their formulation as trisubstituted macrocycle derivatives. The NMR spectra of $H_3N_{3\text{-}F}[9]N_3$ and $H_3N_3[11]N_3$ reveal C_{3v} and C_{2v} symmetry, respectively, compatible with fast nitrogen inversion of the macrocyclic amines. On the other hand, in the proton spectra of **3** and **4** the macrocyclic resonances are split into two groups that were identified by NOE difference experiments as the protons pointing towards the $SiMe_2$ pendant arm groups (H_{syn}) and opposite to them (H_{anti}). The differentiation between *syn* and *anti* protons is indicative of the coordination of the macrocyclic amines to the

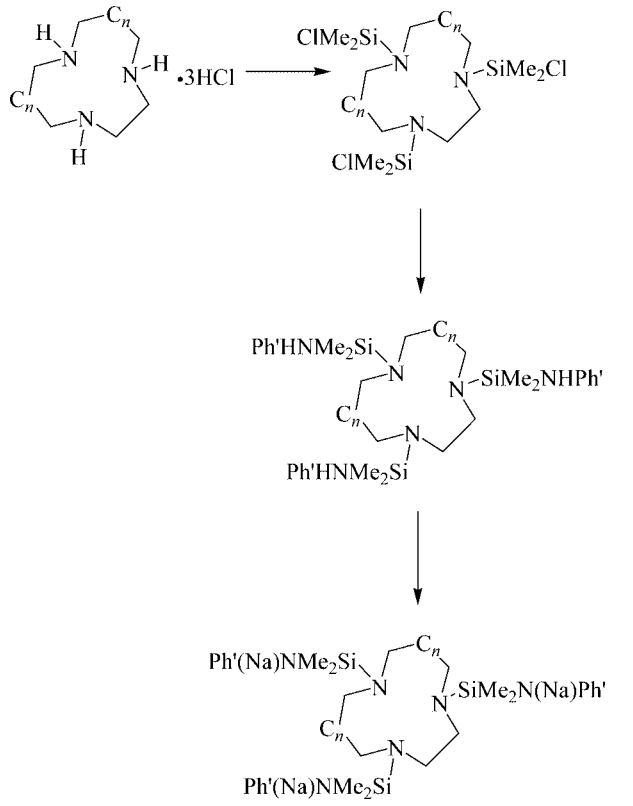

Scheme 1. Syntheses of triazacyclononane and triazacycloundecane ligand precursors. C_n = 0, 1; Ph′ = C_6H_5, *o*-C_6H_4F.

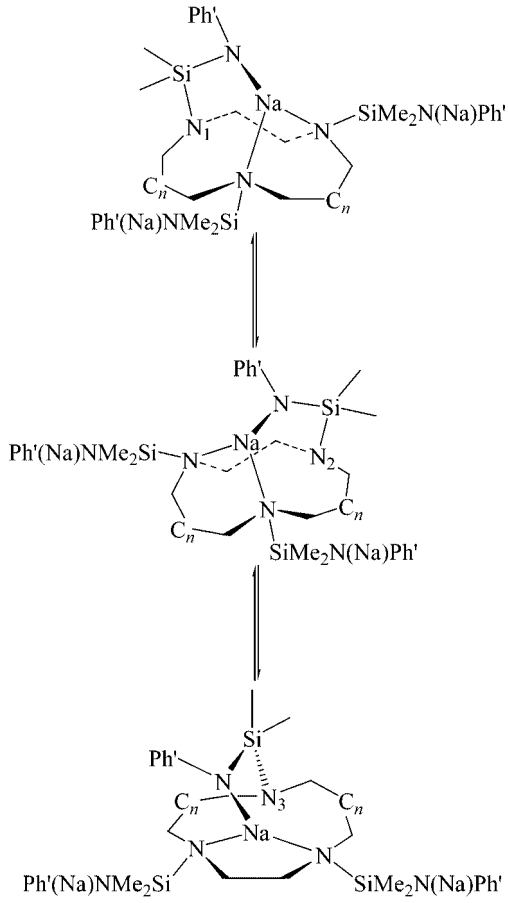

Scheme 2. Fluxional process responsible for the average C_3 and C_s symmetry of **3** and **4**, respectively. C_n = 0, 1; Ph′ = C_6H_5, *o*-C_6H_4F.

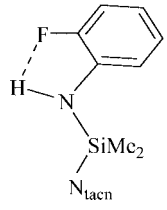

Scheme 3.

sodium cations and attests that, in these conditions, the macrocycle nitrogen inversion is slow on the NMR timescale. Although we have not been able to grow crystals of $Na_3(THF)_2N_{3\text{-}F}[9]N_3$ and $Na_3(THF)_2N_3[11]N_3$ suitable for X-ray structural determination, the similarity between the ^1H and ^{13}C NMR spectra of these compounds and those of $Li_3(THF)_2N_3[9]N_3$ suggests that, in solution, comparable fluxional processes take place.[9] As shown in Scheme 2, the fast exchange between the metals that occupy endocyclic and exocyclic positions creates average C_3 and C_s symmetries for **3** and **4**, respectively. In the case of the tacn derivative **3** this process makes all the pendant arms and macrocyclic carbons equivalent, but for **4**, two sets of resonances owing to the pendant arms (integrating 2:1) and four carbon macrocyclic resonances result. The ^{19}F NMR spectrum of **1** shows a doublet at δ = –57.5 ppm, with coupling constant of 3.9 Hz that results from the coupling with the NH groups through the intramolecular formation of five-membered rings, as represented in Scheme 3.

Treatment of $[TiCl_3(THF)_3]$ with one equivalent of $Na_3(THF)_2N_{3\text{-}F}[9]N_3$ or $Na_3(THF)_2N_3[11]N_3$ in toluene led to the synthesis of $[Ti\{N(2\text{-}FPh)SiMe_2\}_3(tacn)]$ (**5**, $[Ti\{N_{3\text{-}F}[9]N_3\}]$) and $[Ti\{N(Ph)SiMe_2\}_3(tacu)]$ (**6**, $[Ti\{N_3[11]N_3\}]$), respectively (Scheme 4). As expected for paramagnetic compounds, the ^1H NMR spectra of **5** and **6** show broad resonances for all the protons. Large paramagnetic shifts are observed for the macrocyclic protons adjacent to the nitrogens that appear at δ = 5.31 ppm in **5** and δ = 6.27 ppm in **6**. The EPR spectrum of a crystal of **5** at room temperature consists of a symmetrical single line. In solution, at 22 K, a more complex spectrum with g_{av} = 1.953 is obtained, whose hyperfine structure may arise from coupling with fluorine or with ^{47}Ti and ^{49}Ti. The spectral resolution does not allow us to estimate a coupling constant but it is likely that it results from electron coupling to ^{19}F given that coupling to titanium isotopes is rarely observed and has not been detected in the EPR spectrum of the non-fluorinated analogue $[Ti\{N_3[9]N_3\}]$.[9] The solution EPR spectrum of **6** at 298 K shows a symmetrical single line, with g_{av} = 1.944.

Orange crystals of **5** and **6** were grown from toluene solutions at 4 °C. ORTEP illustrations of their molecular structures, as determined by single-crystal X-ray diffraction, are represented in Figure 1 and Figure 2, respectively, and corresponding selected bond length and angles are listed in Table 1 and Table 2.

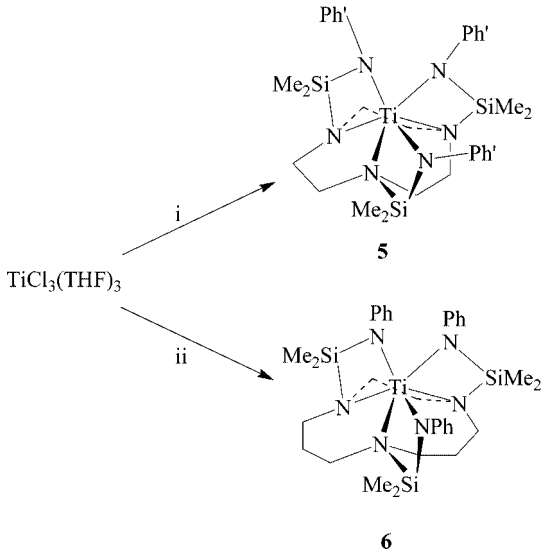

Scheme 4. i) $Na_3N_{3\text{-}F}[9]N_3$, Ph′ = *o*-C_6H_4F; ii) $Na_3N_3[11]N_3$.

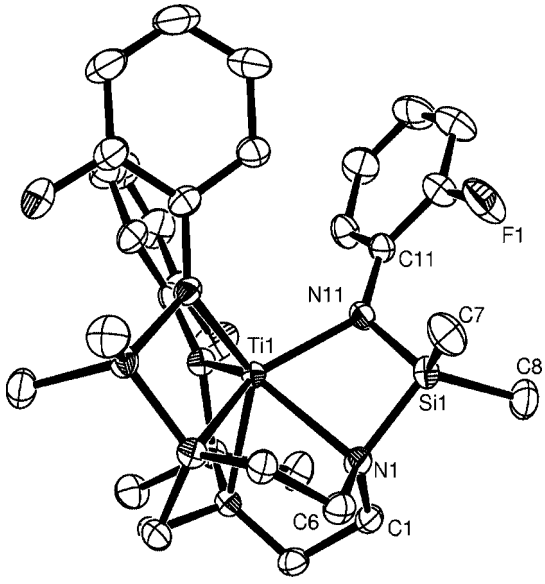

Figure 1. Molecular diagram of compound **5** showing the atomic labelling scheme (ellipsoids at 30% probability level).

In both compounds the metal coordination geometry is best described as distorted trigonal prismatic with three triazamacrocyclic amines and three pendant arm amides bonded to the titanium. Complex **5** crystallizes in the cubic space group $P2_13$ with twist angles between the amide and amine fragments, ϑ, defined by the dihedral angles N_{amino}–cent1–cent2–N_{amido} {N_{amine} and N_{amide} belong to the same pendant arm and cent1 and cent2 are the dummy centroid atoms defined respectively by the three N_{amine} [N(1), N(2), N(3)] and the three N_{amide} atoms [N(11), N(21), N(31)]}[11] of –8.4°, whereas **6** crystallizes in the triclinic space group $P\bar{1}$ with twist angles of –21.1°, –25.8° and –32.2°. The angle between the N(1)–N(2)–N(3) and N(11)–N(21)–N31 planes is 5.5° and the angle cent1–Ti–cent2 is 176.5° for **6** and, obviously, 0° and 180° for **5**. The higher asymmetry reflected by these angles when compared to tacn analogues is

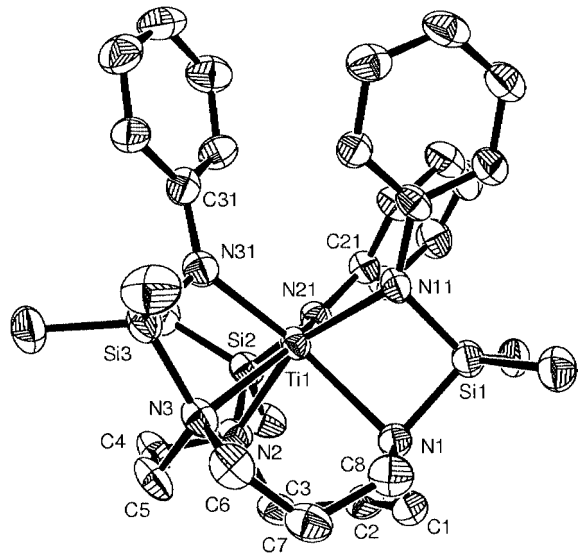

Figure 2. Molecular diagram of compound **6** showing the atomic labelling scheme (ellipsoids at 30% probability level).

a consequence of the different lengths of the tacu methylenic chains.

The distances between the metal and the N_{amine} and N_{amide} planes are 1.65 Å and 0.88 Å in **5** and 1.15 Å and 0.91 Å in **6**, respectively. The longer Ti–N_{tacn} distances compared to Ti–N_{tacu} show the ability of the larger macrocycle chains to adapt to the metal–nitrogen bonding requirements.[14] As it has a larger cavity, the triazacycloundecane ring accommodates the metal cation better than triazacyclononane and thus the metal–amine bonds become shorter. The cooperative effects between the two types of donor fragments is well expressed by the Ti–N_{amide} bond lengths, which follow the opposite trend; that is, the Ti–N_{amide} distances in **5** are shorter than those in **6**. The metal–nitrogen bond length variations are accompanied by different N(i)–Si(i)–N(ij) angles, which are slightly larger in **6** than in **5**. A comparison between the molecular structural parameters of [Ti{$N_{3\text{-}F}[9]N_3$}] and [Ti{$N_3[9]N_3$}] shows that the introduction of the fluorides do not alter the metal···ligand distances significantly, nor the overall coordination geometry. However, the close F···H contacts with the $Si(CH_3)_2$ hydrogens (2.30 Å and 2.73 Å) found in **5** might have induced a more constrained structure than that of [Ti{$N_3[9]N_3$}], thus inducing the crystallization in the cubic space group. Other differences between the two complexes refer to the stereochemical conformation of the TiN-$(CH_2)_2$N metallacycles and to the orientation of the shift between the N_{amido} and N_{amine} planes that is expressed by the twist angles defined above. The configuration of [Ti{$N_3[9]N_3$}] in the solid state was shown to be Δ(λλλ)/Λ(δδδ) whereas that of **5** is Λ(λλλ)/Δ(δδδ).

The two six-membered metallacycles defined by the titanium and the NC_3N chains in **6** display different conformations. The TiN(1)C(8)C(7)C(9)N(3) ring defines a chair conformation while Ti(N1)C(1)C(2)C(3)N(2) has a boat conformation. These arrangements have also been found in [Cu(tacu)Br_2] which is, according to a search performed in

Table 1. Selected bond lengths [Å] and angles [°] for [Ti{$N_{3\text{-}F}$[9]N_3}] (**5**) and [Ti{$N_{3\text{-}F}$[9]N_3}]I (**7**).

	5	**7**
Ti(1)–N(1)	2.326(3)	2.262(14)
Ti(1)–N(2)	–	2.259(13)
Ti(1)–N(3)	–	2.266(15)
Ti(1)–N(11)	2.078(2)	1.987(13)
Ti(1)–N(21)	–	1.997(13)
Ti(1)–N(31)	–	1.969(12)
N(1)–C(1)	1.490(4)	1.550(18)
Plane[N(1)–N(2)–N(3)]–Ti(1)	1.65(7)	1.60(9)
Plane[N(11)–N(21)–N(31)]–Ti(1)	0.88(7)	0.85(9)
N(1)–Ti(1)–N(11)	70.59(10)	70.1(5)
N(2)–Ti(1)–N(21)	–	72.5(5)
N(3)–Ti(1)–N(31)	–	70.8(5)
N(1)–Ti(1)–N(2)	75.21(10)	75.1(5)
N(2)–Ti(1)–N(3)	–	75.4(5)
N(3)–Ti(1)–N(1)	–	75.8(5)
N(11)–Ti(1)–N(21)	103.45(9)	103.5(5)
N(11)–Ti(1)–N(31)	–	103.0(6)
N(21)–Ti(1)–N(31)	–	104.5(5)
Plane[N(1)–N(2)–N(3)]–Plane[N(11)–N(21)–N(31)]	0	1.6
[N(1)–N(2)–N(3)][a]–Ti(1)–[N(11)–N(21)–N(31)][a]	180	178.1
N(1)–[N(1)–N(2)–N(3)][a]–[N(11)–N(21)–N(31)][a]–N(11)	–8.4	+ 16.3
N(2)–[N(1)–N(2)–N(3)][a]–[N(11)–N(21)–N(31)][a]–N(21)	–	+15.0
N(3)–[N(1)–N(2)–N(3)][a]–[N(11)–N(21)–N(31)][a]–N(31)	–	+ 14.4

[a] Centroid defined by the atoms in brackets.

Table 2. Selected bond lengths [Å] and angles [°] for one of the molecules of [Ti{N_3[11]N_3}] (**6**).

[Ti{N_3[11]N_3}]	
Ti(1)–N(1)	2.340(6)
Ti(1)–N(2)	2.311(5)
Ti(1)–N(3)	2.425(6)
Ti(1)–N(11)	2.074(5)
Ti(1)–N(21)	2.064(6)
Ti(1)–N(31)	2.057(6)
Plane[N(1)–N(2)–N(3)]–Ti(1)	1.48(3)
Plane[N(11)–N(21)–N(31)]–Ti(1)	0.90(3)
N(1)–Ti(1)–N(11)	70.1(2)
N(2)–Ti(1)–N(21)	70.8(2)
N(3)–Ti(1)–N(31)	69.3(2)
N(1)–Ti(1)–N(2)	90.1(2)
N(2)–Ti(1)–N(3)	74.7(2)
N(3)–Ti(1)–N(1)	86.9(2)
N(11)–Ti(1)–N(21)	100.0(2)
N(11)–Ti(1)–N(31)	101.4(2)
N(21)–Ti(1)–N(31)	105.7(2)
Plane[N(1)–N(2)–N(3)]–Plane[N(11)–N(21)–N(31)]	5.5 (3)
[N(1)–N(2)–N(3)][a]–Ti(1)–[N(11)–N(21)–N(31)][a]	176.5(9)
N(1)–[N(1)–N(2)–N(3)][a]–[N(11)–N(21)–N(31)][a]–N(11)	–25.8(10)
N(2)–[N(1)–N(2)–N(3)][a]–[N(11)–N(21)–N(31)][a]–N(21)	–32.2(12)
N(3)–[N(1)–N(2)–N(3)][a]–[N(11)–N(21)–N(31)][a]–N(31)	–21.1(10)

[a] Centroid defined by the atoms in brackets.

CCDC, the only triazacycloundecane complex characterised by X-ray diffraction.[15]

Treatment of **5** and **6** with iodine gave the corresponding Ti^{IV} derivatives [Ti{$N_{3\text{-}F}$[9]N_3}]I (**7**) and [Ti{N_3[11]N_3}]I (**8**). The ^{1}H NMR spectrum of **7** is compatible with an average C_3 symmetry in solution where the macrocyclic protons appear as two sets of resonances attributable to H_{syn} and H_{anti}. The ^{19}F NMR spectrum shows a broad singlet at δ = –41.2 ppm.

The molecular structure of **7** is depicted in Figure 3 and selected bond lengths and angles are reported in Table 1.

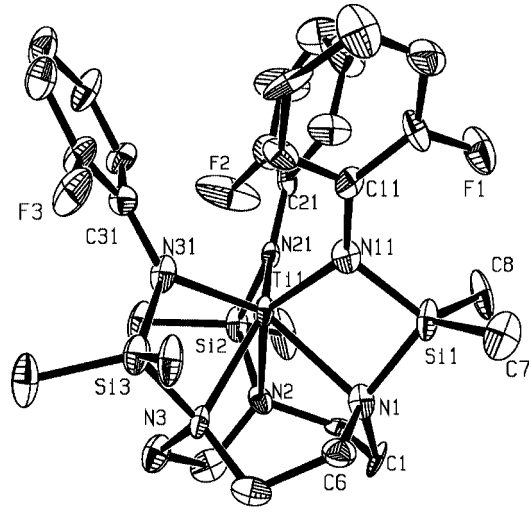

Figure 3. Molecular diagram of the cation of compound **7** showing the atomic labelling scheme (ellipsoids at 30% probability level).

In **7**, the titanium coordination geometry is best described as distorted trigonal prismatic with twist angles, ϑ, of 14.4°, 15.0° and 16.3°. The angle between the N(1)–N(2)–N(3) and N(11)–N(21)–N(31) planes is 1.6° and the angle cent1–Ti–cent2 is 178.1°. The amide nitrogen atoms are planar, with a sum of the angles around them of 359.6° for N(11), 359.8° for N(21) and 360.0° for N(31). The Ti–N_{amine} bond lengths range between 2.259 and 2.266 Å and the Ti–N_{amide} vary from 1.969 to 1.997 Å (see Table 1). Although slightly shorter than the values obtained for the Ti^{III}

starting material, the metal···nitrogen distances in **7** are close to those found in cations $[Ti\{N_3[9]N_3\}]X$ (X = I, BPh_4), denoting that, once more, the *ortho*-fluorines have no significant influence on the ligand coordination. Similarly to **5**, short F···H distances (2.27–2.38 Å) between the fluoride and the $SiMe_2$ groups of each pendant arm are observed for **7**. The configuration of the five-membered $TiNC_2N$ metallacycles in **7** is the same as for **5** [Λ(λλλ)/Δ(δδδ)].

In CD_2Cl_2, at room temperature, the ^1H NMR spectrum of $[Ti\{N_3[11]N_3\}]I$ (**8**) is consistent with an average C_s symmetry, displaying two sets of aromatic resonances corresponding to the phenyl rings and three singlets for the six CH_3 groups of the bridging dimethylsilyl groups. The C_2-chain methylenic protons lead to different H_{syn} and H_{anti} resonances at δ = 3.39 and 3.68 ppm, respectively, and the C_3-chain protons give rise to four multiplets centred at δ = 2.37 and 2.05 ppm, corresponding to the H_{syn} and H_{anti} protons of the middle of the chain, and at δ = 3.47 and 3.30 ppm corresponding to the H_{syn} and H_{anti} protons adjacent to the nitrogen atoms. This pattern reveals that the three exchange processes available to the molecule at room temperature, namely the trigonal twist of the N_{amine} and N_{amide} planes, which corresponds to the equilibrium between the two possible enantiomers Δ and Λ, the δ/λ interconversion of the five-membered metallacycle and the chair/boat interconversion are fast processes on the NMR timescale (Scheme 5). At –40 °C, the dimethylsilyl protons split into five singlets and the three phenyl rings become non-equivalent, implying that the δ/λ isomerisation is blocked at that temperature. The C_2 macrocyclic protons pattern broadens as a consequence of the splitting into an ABCD system that partially overlaps the C_3 chain resonances. The two other fluxional processes are still operative, as revealed by the equivalence of the two methyl groups of the pendant arm bonded to the nitrogen between the two C_3 macrocyclic chains. At –70 °C these protons also become non-equivalent. Six different methyl resonances and the appearance of a series of interpenetrating multiplets due to non-equivalent macrocyclic protons are indicative that the equilibrium between the two enantiomers is blocked.

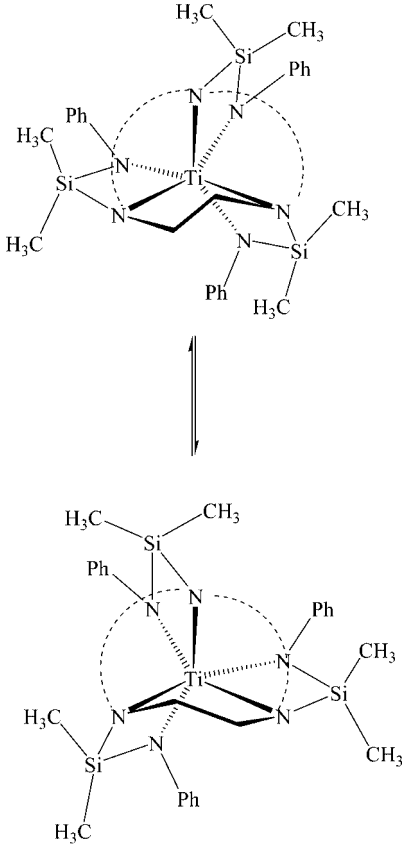

Scheme 5. Exchange processes responsible for the average C_s symmetry of $[Ti\{N_3[11]N_3\}]I$ (**8**).

To evaluate the donor ability of the $N_3[9]N_3$ and $N_{3\text{-}F}[9]N_3$ sets used we performed cyclic voltammetry measurements of complexes $[Ti\{N_{3\text{-}F}[9]N_3\}]$ (**5**), $[Ti\{N_{3\text{-}F}[9]N_3\}]I$ (**7**) and $[Ti\{N_3[9]N_3\}]X$ (X = I, **9**, BPh_4, **10**)[9] in acetonitrile at variable scan rates. The results are listed in Table 3.

Table 3. Electrochemical data for complexes **5**, **7**, **9** and **10**.

Compound[a]	$E^{red}_{1/2}$ [V]	$E^{ox}_{1/2}$ [V]	Solvent
$[Ti\{N_{3\text{-}F}[9]N_3\}]$		–1.59	CH_3CN
$[Ti\{N_{3\text{-}F}[9]N_3\}]I$	–1.58	–0.22	CH_3CN
$[Ti\{N_3[9]N_3\}]\ BPh_4$	–1.71		CH_3CN
	–1.78		CH_2Cl_2
$[Ti\{N_3[9]N_3\}]I$	–1.71	–0.20	CH_3CN

[a] At 25 °C, 6.5×10^{-2} M $(Bu_4N)BPh_4$, 10^{-3} M $FeCp_2$. All potentials were recorded at 200 mV s^{-1}.

The first remark concerns the stability of the different complexes in the medium. Triazacycloundecane derivatives are, in general, less stable than the triazacyclononane-based complexes and this characteristic prevents their study by cyclic voltammetry. The stability of the cations is higher than that of the reduced metal complexes and thus $[Ti\{N_3[9]N_3\}]$ and $[Ti\{N_3[11]N_3\}]$ are not suitable starting materials for CV measurements. Remarkably, $[Ti\{N_{3\text{-}F}[9]N_3\}]$ is much more stable than the other Ti^{III} compounds and, in acetonitrile, a reversible one-electron oxidation at $E^{ox}_{1/2}$ = –1.59 V was detected at a scan rate of 200 mV s^{-1}. Cationic tacn derivatives show reversible one-electron reduction peaks. Figure 4 shows the cyclic voltammogram of $[Ti\{N_3[9]N_3\}]BPh_4$ (**10**) as an example.

The values listed in Table 3 show that the redox potentials for the Ti^{IV}/Ti^{III} couple in complexes **9** and **10** are lower than the values reported for metallocene titanium dichlorides such as $[Cp_2TiCl_2]$, $[Cp^*_2TiCl_2]$ and $[(C_5H_4SiMe_3)_2TiCl_2]$, for which $E^{red}_{1/2}$ values range from –1.295 to –1.621 mV.[16–18] On the other hand, the value of –1.58 mV measured for $E^{red}_{1/2}$ of **7** reflects the additional stability of the LUMO when C_6H_5 is replaced by *o*-C_6H_4F. The similarity between the reduction potential of **7** and that of $[Ti\{O_3[9]N_3\}]PF_6$ ($H_3O_3[9]N_3$ = 1,4,7-tris(5-*tert*-butyl-2-hydroxybenzyl)-1,4,7-triazacyclononane; $E^{red}_{1/2}$ = –1.52 mV) shows that the donor ability of the amide moieties in **7** is comparable to that of the alkoxide fragments in $[Ti\{O_3[9]N_3\}]PF_6$.[17] The voltammograms of **7** and **9** display addition redox

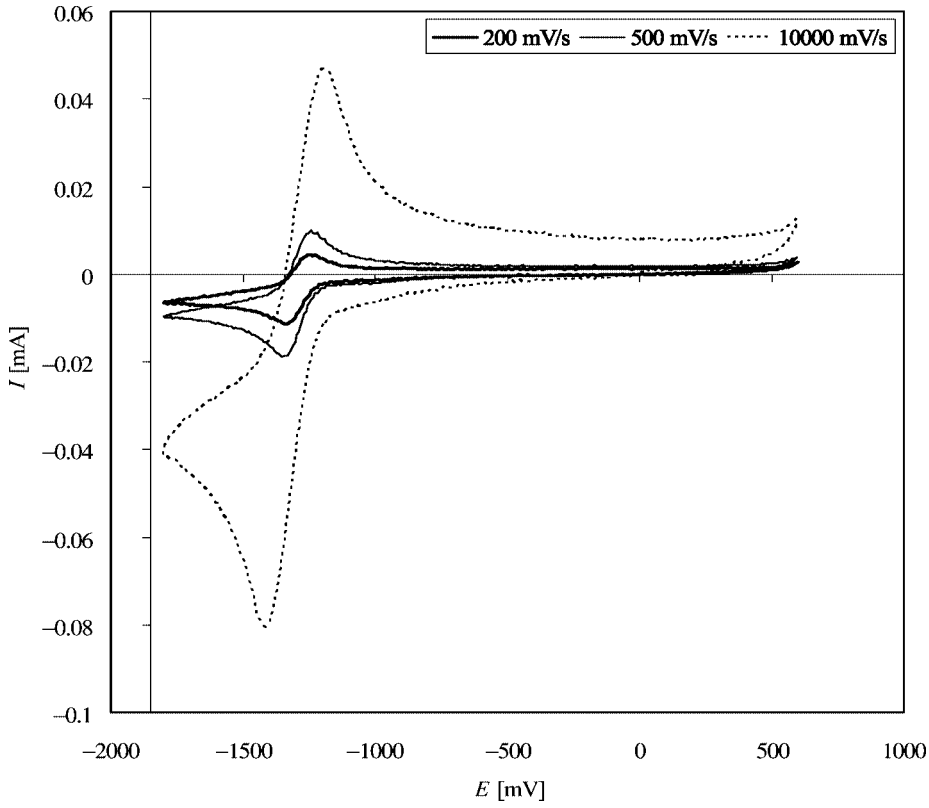

Figure 4. Cyclic voltammogram of [Ti{N_3[9]N_3}]BPh_4 (**10**) in [Bu_4N]BPh_4/CH_3CN, at scan rates of 200 mV s^{-1}, 500 mV s^{-1} and 1000 mV s^{-1}.

peaks at –0.22 V and –0.20 V, respectively, that are due to the I^- counterion.

Experimental Section

General Procedures and Starting Materials: All reactions were conducted under a nitrogen atmosphere. Solvents were pre-dried with 4 Å molecular sieves and refluxed over sodium-benzophenone (diethyl ether, tetrahydrofuran, *n*-hexane and toluene) or calcium hydride (dichloromethane) under an atmosphere of nitrogen, and collected by distillation. Deuterated solvents were dried with molecular sieves and freeze-pump-thaw degassed prior to use. Proton (300 MHz) and carbon (75.419 MHz) NMR spectra were recorded with a Varian Unity 300, at 298 K, unless stated otherwise. The spectra are referenced to internal residual protio-solvent (^1H) or solvent (^{13}C) resonances and reported relative to tetramethylsilane (δ = 0 ppm). Assignments were supported by NOE difference experiments and by ^{13}C-^1H hetero-correlations, as appropriate. EPR spectra were recorded at room temperature with a Bruker 300E spectrometer at X-band frequency ($\nu \approx 9.5$ GHz). Mass spectra were performed at the Laboratoire de Spectrométrie de Masse, Université de Rouen, France. Elemental analyses were obtained from the Laboratório de Análises do IST, Lisbon, Portugal.

Triethylamine, aniline, $SiMe_2Cl_2$, $TiCl_3$ and NaH (60% dispersion in mineral oil) were purchased from Aldrich. NEt_3 and NH_2Ph were pre-dried with molecular sieves, refluxed over calcium hydride, and collected by distillation. $SiMe_2Cl_2$ was purified by removal of residual HCl and then distilled trap-to-trap. NaH was washed with THF prior to use. [$TiCl_3(THF)_3$],[19] tacn·3HCl,[11] tacu·3HCl,[12] and 1,4,7-$(SiMe_2Cl)_3$-tacn[9] were prepared according to described procedures.

Cyclic voltammetric measurements were carried out with a Radiometer DEA 101 Digital Electrochemical Analyser interfaced with an IMT 102 Electrochemical Interface. [Bu_4N][BPh_4] (Fluka, electrochemical grade) was used as supporting electrolyte in CH_2Cl_2 or CH_3CN with a concentration of 6.5×10^{-2} M. All experiments were performed with concentrations of complexes in the range 2–4×10^{-3} M. All potentials are referenced to the ferrocene/ferrocenium couple as internal standard with $E_{1/2}$ = 0.50 V vs. S.C.E. A Pt disc (φ = 1 mm) was used as working electrode. The solvents were distilled immediately before use. All experiments were carried out at 25 °C in the absence of oxygen. Dry nitrogen was bubbled through the solution in the cell before measurements.

1,4,7-[{N(H)(2-C_6H_4F)}$SiMe_2$]$_3$-tacn (1): 2-Fluoraniline (2.1 mL, 21.9 mmol) was added to a suspension of NaH (0.95 g, 39.6 mmol) in THF. The mixture was heated to 60 °C and stirred for 12 h. The excess of NaH was filtered off and washed with 20 mL of THF, at room temperature. The filtrates were added dropwise to a solution of 1,4,7-$(SiMe_2Cl)_3$-tacn (2.74 g, 6.74 mmol) in toluene (80 mL), cooled to –40 °C. The mixture was warmed to room temperature and stirred for 12 h. The solvents were evaporated and the residue was extracted in hexane and filtered. Evaporation to dryness led to a very viscous yellow oil in quantitative yield (4.25 g). ^1H NMR (C_6D_6): δ = 6.94–6.90 (m, 3 H, H_{meta}), 6.88–6.87 (m, 3 H, H_{meta}), 6.85–6.82 (m, 3 H, H_{ortho}), 6.55–6.48 (m, 3 H, H_{para}), 3.77 (d, $J_{H,F}$ = 3.9 Hz, 3 H, N*H*), 2.89 (s, 12 H, NCH_2CH_2N), 0.09 (s, 18 H, CH_3) ppm. $^{13}C\{^1H\}$ NMR (C_6D_6): δ = 153.1 (d, $^1J_{C,F}$ = 236.0 Hz, C_{ortho}), 135.8 (d, $^2J_{C,F}$ = 13.0 Hz, C_{ipso}), 124.8 (d, $^4J_{C,F}$ = 3.5 Hz, C_{meta}), 118.0 (d, $^3J_{C,F}$ = 7.0 Hz, C_{para}), 117.2 (d, $^3J_{C,F}$ = 3.5 Hz,

C$_{ortho}$), 115.3 (d, $^2J_{C,F}$ = 20.0 Hz, *C*$_{meta}$), 50.5 (N*C*H$_2$*C*H$_2$N), –1.4 (*C*H$_3$) ppm. ^{19}F NMR (C$_6$D$_6$): δ = –57.47 ppm. $C_{30}H_{45}N_6F_3Si_3$ (630.98): calcd. C 57.08, H 7.19, N 13.33; found C 57.06, H 7.20, N 13.20. MS (EI): *m*/*z* = 630 [M]$^+$.

1,4,8-[SiMe$_2$Cl]$_3$-tacu: A suspension of tacu·3HCl (1.06 g, 3.97 mmol) in CH_2Cl_2 (50 mL), cooled to 0 °C, was treated with Et_3N (6,0 mL, 40 mmol). The mixture was stirred during 15 minutes and $SiMe_2Cl_2$ (3.0 mL, 24 mmol) was added. The reaction proceeded overnight at room temperature and a precipitate formed. The volatiles were then evaporated under vacuum and the residue was extracted with hexane and filtered. Evaporation of the hexane led to a white solid in quantitative yield (1.72 g). The reaction was scaled up to 20 mmol of tacu·3HCl. ^{1}H NMR (C$_6$D$_6$): δ = 2.90 (s, 4 H, NC*H*$_2$C*H*$_2$N), 2.83 [t, $^3J_{H,H}$ = 6.9 Hz, 4 H, N(CH$_2$)$_2$C*H*$_2$N(CH$_2$)$_2$N], 2.65 [t, $^3J_{H,H}$ = 6.9 Hz, 4 H, (CH$_2$)$_2$-C*H*$_2$NC*H*$_2$(CH$_2$)$_2$], 1.53 (quint., $^3J_{H,H}$ = 6.9 Hz, 4 H, NCH$_2$C*H*$_2$CH$_2$N), 0.29 (s, 12 H, SiC*H*$_3$), 0.27 (s, 6 H, SiC*H*$_3$) ppm. ^{13}C{^{1}H} NMR (C$_6$D$_6$): δ = 50.4 (N*C*H$_2$*C*H$_2$N), 46.2 [(CH$_2$)$_2$*C*H$_2$-N*C*H$_2$(CH$_2$)$_2$], 45.7 [N(CH$_2$)$_2$*C*H$_2$N(CH$_2$)$_2$N], 30.8 (NCH$_2$*C*H$_2$-CH$_2$N), 2.3 [(CH$_2$)$_3$N{Si(*C*H$_3$)$_2$}(CH$_2$)$_3$], 2.1 [(CH$_2$)$_3$N{Si(*C*H$_3$)$_2$}-(CH$_2$)$_2$] ppm. $C_{14}H_{34}N_3Cl_3Si_3$ (435.06): calcd. C 38.63, H 7.88, N 9.66; found C 38.55, H 7.96, N 9.55. MS (EI): *m*/*z* = 401 [M – Cl]$^+$.

1,4,8-[N(H)(C$_6$H$_5$)SiMe$_2$]$_3$-tacu (2): PhNH$_2$ (6.8 mL, 74 mmol) was added at 0 °C to a suspension of NaH (2.32 g, 93 mmol) in 100 mL of THF. The cooling bath was removed and, once the initial effervescence had stopped, the mixture was warmed at 60 °C for 12 h. The solution was filtered and the residue washed with THF (20 mL). The solution was transferred dropwise, at –40 °C, to a solution of 1,4,8-[ClSiMe$_2$]$_3$-tacu (10.24 g, 23.54 mmol) in 100 mL of toluene. The reaction took place at room temperature during 12 h and the volatiles were then evaporated. The residue was extracted with hexane and filtered off. Evaporation of the solvent led to 14.23 g of **2** (100%). ^{1}H NMR (C$_6$D$_6$): δ = 7.20–7.13 (m, 6 H, *H*$_{meta}$), 6.81–6.73 (m, 3 H, *H*$_{para}$), 6.67 (d, $^3J_{H,H}$ = 8.9 Hz, 4 H, *H*$_{ortho}$), 6.60 (d, $^3J_{H,H}$ = 8.9 Hz, 2 H, *H*$_{ortho}$), 3.15 (s, 2 H, N*H*), 3.12 (s, 1 H, N*H*), 3.02 (s, 4 H, NC*H*$_2$C*H*$_2$N), 2.73 [t, $^3J_{H,H}$ = 6.9 Hz, 4 H, (CH$_2$)$_2$C*H*$_2$NC*H*$_2$(CH$_2$)$_2$], 2.39 [t, $^3J_{H,H}$ = 6.9 Hz, 4 H, N(CH$_2$)$_2$C*H*$_2$N(CH$_2$)$_2$N], 1.63 (quint., $^3J_{H,H}$ = 6.9 Hz, 4 H, NCH$_2$C*H*$_2$CH$_2$N), 0.12 (s, 12 H, SiC*H*$_3$), 0.08 (s, 6 H, SiC*H*$_3$) ppm. ^{13}C{^{1}H} NMR (C$_6$D$_6$): δ = 147.4 (3 C, *C*$_{ipso}$), 129.5 (2 C, C$_{meta}$), 129.4 (4 C, C$_{meta}$), 118.3 (2 C, C$_{para}$), 118.2 (1 C, C$_{para}$), 116.9 (4 C, C$_{ortho}$), 116.8 (2 C, C$_{ortho}$), 50.2 (N*C*H$_2$*C*H$_2$N), 46.7 [(CH$_2$)$_2$*C*H$_2$N*C*H$_2$(CH$_2$)$_2$], 45.3 [N(CH$_2$)$_2$*C*H$_2$N(CH$_2$)$_2$N], 32.0 (NCH$_2$*C*H$_2$CH$_2$N), –1.05 [(CH$_2$)$_3$N{Si(*C*H$_3$)$_2$}(CH$_2$)$_3$], –1.08 [(CH$_2$)$_3$N{Si(*C*H$_3$)$_2$}(CH$_2$)$_2$] ppm. $C_{32}H_{52}N_6Si_3$ (605.06): calcd. C 63.50, H 8.67, N 13.90; found C 63.75, H 8.61, N 13.86. MS (EI): *m*/*z* = 604 [M]$^+$.

[1,4,7-{N(Na)(2-C$_6$H$_4$F)SiMe$_2$}$_3$-tacn]·2THF (3): A solution of 1,4,7-{[N(H)(2-C$_6$H$_4$F)]SiMe$_2$}$_3$-tacn (7.91 g, 12.54 mmol) in THF (25 mL) was added dropwise to a suspension of NaH (1.2 g, 50 mmol) in THF (100 mL). The mixture was then heated at 60 °C for 12 h. The solution was filtered off and the excess of NaH was washed with THF (30 mL). Evaporation of the THF led to a greenish solid in quantitative yield (10.54 g). ^{1}H NMR (C$_6$D$_6$): δ = 6.94 (m, 6 H, *H*$_{ortho}$, *H*$_{meta}$), 6.84 (t, $^3J_{H,H}$ = 6.6 Hz, 3 H, *H*$_{meta}$), 6.24 (m, 3 H, *H*$_{para}$), 3.41 (m, 8 H, OC*H*$_2$, THF), 3.07–2.95 (m, 6 H, C*H*$_2$, *syn*), 2.75–2.63 (m, 6 H, C*H*$_2$, *anti*), 1.30 (m, 8 H, C*H*$_2$, THF), 0.28 (s, 18 H, C*H*$_3$) ppm. ^{13}C{^{1}H} NMR (C$_6$D$_6$): δ = 158.1 (d, $^1J_{C,F}$ = 225.0 Hz, *C*$_{ortho}$), 149.5 (br., *C*$_{ipso}$), 125.1 (*C*$_{meta}$), 124.3 (*C*$_{ortho}$), 114.4 (d, $^2J_{C,F}$ = 24.0 Hz, *C*$_{meta}$), 110.3 (*C*$_{para}$), 67.9 (OCH$_2$, THF), 48.3 (NCH$_2$CH$_2$N), 25.6 (*C*H$_2$, THF), 0.1 (*C*H$_3$) ppm. ^{19}F NMR(C$_6$D$_6$): δ = –63.24 (m) ppm.

1,4,8-[{N(Na)(C$_6$H$_5$)SiMe$_2$}$_3$-tacu]·2THF (4): A solution of 1,4,8-[N(H)(C$_6$H$_5$)SiMe$_2$]$_3$-tacu (7.03 g, 11.62 mmol) in THF (ca. 25 mL) was added to a suspension of NaH (1.00 g, 42 mmol) in 100 mL of THF. The mixture was slowly warmed to 60 °C and stirred at this temperature for 12 h. After cooling to room temperature, the solution was filtered off and the NaH excess was washed with 30 mL of THF that was collected with the filtrate. The solvent was evaporated to dryness and a greenish powder was obtained by scratching the dried material under N_2, at liquid nitrogen temperature. Yield: 8.63 g, quantitative. ^{1}H NMR (C$_6$D$_6$): δ = 7.16 (t, $^3J_{H,H}$ = 7.2 Hz, 2 H, *H*$_{meta}$), 7.07 (t, $^3J_{H,H}$ = 6.9 Hz, 4 H, *H*$_{meta}$), 6.76 (t, $^3J_{H,H}$ = 7.2 Hz, 6 H, *H*$_{ortho}$), 6.58 (t, $^3J_{H,H}$ = 7.2 Hz, 1 H, *H*$_{para}$), 6.47 (t, $^3J_{H,H}$ = 6.9 Hz, 2 H, *H*$_{para}$), 3.27 (m, 8 H, OC*H*$_2$, THF), 2.86 [br. s, 6 H, NC*H*$_{syn}$H$_{anti}$CH$_2$C*H*$_{syn}$H$_{anti}$N(C*H*$_{syn}$H$_{anti}$)$_2$N], 2.56 [br. s, 2 H, N(CH$_{syn}$*H*$_{anti}$)$_2$N], 2.44 (br. s, 4 H, NCH$_{syn}$*H*$_{anti}$CH$_2$CH$_{syn}$-*H*$_{anti}$N), 1.67 (br. s, 2 H, NCH$_2$C*H*$_{syn}$H$_{anti}$CH$_2$N), 1.38 (br. s, 2 H, NCH$_2$CH$_{syn}$*H*$_{anti}$CH$_2$N), 1.24 (m, 8 H, C*H*$_2$, THF), 0.34 (s, 6 H, SiC*H*$_3$), 0.29 (s, 12 H, SiC*H*$_3$) ppm. ^{13}C{^{1}H} NMR (C$_6$D$_6$): δ = 161.1 (1 C, *C*$_{ipso}$), 160.4 (2 C, *C*$_{ipso}$), 130.7 (4 C, *C*$_{meta}$), 130.2 (2 C, *C*$_{meta}$), 122.9 (2 C, *C*$_{ortho}$), 121.8 (4 C, *C*$_{ortho}$), 113.3 (1 C, *C*$_{para}$), 113.2 (2 C, *C*$_{para}$), 67.8 (O*C*H$_2$, THF), 51.4 [(CH$_2$)$_2$*C*H$_2$-N*C*H$_2$(CH$_2$)$_2$], 50.7 [N(CH$_2$)$_2$*C*H$_2$N(CH$_2$)$_2$N], 49.0 [N(*C*H$_2$)$_2$N], 30.0 (NCH$_2$*C*H$_2$CH$_2$N), 25.5 (*C*H$_2$, THF), 1.2 [(CH$_2$)$_3$N{Si-(*C*H$_3$)$_2$}(CH$_2$)$_3$], 0.1 [(CH$_2$)$_3$N{Si(*C*H$_3$)$_2$}(CH$_2$)$_2$] ppm.

[Ti{N(2-C$_6$H$_4$F)SiMe$_2$}$_3$-tacn] (5): A solution of [1,4,7-{N(Na)(2-C$_6$H$_4$F)SiMe$_2$}$_3$-tacn]·2THF (2.30 g, 2.86 mmol) in toluene (10 mL) was rapidly added at –60 °C to a suspension of [TiCl$_3$(THF)$_3$] (1.11 g, 3.00 mmol) in toluene (40 mL). The mixture was allowed to warm to room temperature while being stirred for 12 h. The solution was filtered through a celite layer and the residue was washed with toluene and collected together with the filtrate. The solvents were evaporated under vacuum and the compound was washed at –30 °C with hexane (2 × 5 mL). Yield: 90% (1.69 g). ^{1}H NMR (C$_6$D$_6$): δ = 9.25, 7.98, 6.93 (br., 2-C$_6$*H*$_4$F), 5.30 (br., NC*H*$_2$C*H*$_2$N), 0.61 [br., Si(C*H*$_3$)$_2$] ppm. EPR (10^{-2} M in toluene, 22 K): *g* = 1.953. $C_{30}H_{42}F_3N_6Si_3Ti$ (675.82): calcd. C 53.29, H 6.27, N 12.44; found C 53.20, H 6.36, N 12.43. MS (EI): *m*/*z* = 583 [M$^+$ – C$_6$H$_2$F].

[Ti{N(Ph)SiMe$_2$}$_3$-tacu] (6): A suspension of [TiCl$_3$(THF)$_3$] (1.23 g, 3.31 mmol) in 50 mL of toluene was treated at –60 °C with a solution of 1,4,8-[{N(Na)(C$_6$H$_5$)SiMe$_2$}$_3$-tacu]·2THF (2.36 g, 3.18 mmol) in 10 mL of toluene. The mixture was allowed to reach room temperature and was stirred for a further 12 h. The solution was filtered through a celite layer and the solvent evaporated to dryness. The solid obtained was washed at –30 °C with hexane and dried. Crystals suitable for X-ray diffraction were obtained from toluene at 4 °C. Yield: 80% (1.65 g). EPR (10^{-2} M in toluene, 22 K): *g* = 1.944. $C_{32}H_{49}N_6Si_3Ti$ (649.90): calcd. C 59.11, H 7.60, N 12.94; found C 59.03, H 7.73, N 12.88. MS (EI): *m*/*z* = 649 [M]$^+$.

[Ti{N(2-C$_6$H$_4$F)SiMe$_2$}$_3$-tacn]I (7): A solution of [Ti{N(2-C$_6$H$_4$F)SiMe$_2$}$_3$-tacn] (0.80 g, 1.19 mmol) in 40 mL of toluene, cooled to –60 °C, was treated with I_2 (0.15 g, 0.60 mmol). The solution was allowed to warm to room temperature and was then stirred for 12 h. The solvent was evaporated to dryness and the residue was washed with hexane and dried in vacuo to give **7** as an orange solid in 98% yield (0.93 g). ^{1}H NMR (C$_6$D$_5$Br): δ = 7.37 (br. t, 3 H, *H*$_{meta\text{-}H3}$), 7.30–7.20 (m, 3 H, *H*$_{para}$), 6.95 (t, $^3J_{H,H}$ = 6.6 Hz, 3 H, *H*$_{meta\text{-}H5}$), 5.76 (t, $^3J_{H,H}$ = 7.2 Hz, 3 H, *H*$_{ortho}$), 4.65–4.40 (br. s, C*H*$_{anti}$H$_{syn}$), 3.95–3.75 (m, 6 H, CH$_{anti}$*H*$_{syn}$), 0.72 (s, 18 H, C*H*$_3$) ppm; (CD$_3$CN): δ = 7.09 (ddd, $^3J_{H,F}$ = 11.4, $^3J_{H,H}$ = 8.4, $^4J_{H,H}$ = 1.5 Hz, 3 H, *H*$_{meta\text{-}H3}$), 7.02–6.93 (m, 3 H, *H*$_{para}$), 6.52 (dt, $^3J_{H,H}$ = 7.8, $^5J_{H,F}$ = 1.5 Hz, 3 H, *H*$_{meta\text{-}H5}$), 5.43 (dt, $^3J_{H,H}$

Table 4. Crystal and refinement data for compounds **5** and **7**.

	5	**7**
Empirical formula	$C_{30}H_{42}F_3N_6Si_3Ti$	$C_{30}H_{42}F_3IN_6Si_3Ti$
Formula mass	675.87	802.77
Temperature	293(2) K	293(2) K
Wavelength	0.71069 Å	0.71069 Å
Crystal system	cubic	orthorhombic
Space group	$P2_13$	$P21cn$
Unit cell dimensions	a = 15.080(2) Å b = 15.0780(16) Å c = 15.0753(16) Å	a = 10.577(5) Å b = 17.772(5) Å c = 18.911(5) Å
Volume	3427.7(7) Å^3	3555(2) Å^3
Z	4	4
Calculated density	1.310 Mg m^{-3}	1.500 Mg m^{-3}
Absorption coefficient	0.401 mm^{-1}	1.256 mm^{-1}
F(000)	1420	1632
Crystal size	prism	parallelepiped
Crystal morphology	0.5×0.3×0.3 mm	0.6×0.4×0.3 mm
Colour	red	red
Theta range for data collection	1.91 to 26.00°	1.57 to 25.97°
Limiting indices	$0 \le h \le 18$ $0 \le k \le 18$ $-18 \le l \le 18$	$0 \le h \le 13$ $0 \le k \le 21$ $0 \le l \le 23$
Reflections collected/unique	7249/2262 [R(int) = 0.0489]	3603/3603 [R(int) = 0.0000]
Completeness to theta	99.7% (θ = 26.00)	97.8% (θ = 25.97)
Refinement method	full-matrix least-squares on F^2	full-matrix least-squares on F^2
Data/restraints/parameters	2262/0/131	3603/1/392
Goodness-of-fit on F^2	1.073	1.074
Final R indices [$I > 2\sigma(I)$]	$R1$ = 0.0400, $wR2$ = 0.0892	$R1$ = 0.0984, $wR2$ = 0.2247
R indices (all data)	$R1$ = 0.0593, $wR2$ = 0.1007	$R1$ = 0.1365, $wR2$ = 0.2663
Absolute structure parameter	0.46(5)	0.08(7)
Largest diff. peak and hole	0.215 and –0.196 e Å^{-3}	3.954 and –2.026 e Å^{-3}

= 7.8, $^4J_{H,F}$ = 7.8, $^4J_{H,H}$ = 2.1 Hz, 3 H, H_{ortho}), 3.63 (s, 12 H, NCH_2CH_2N), 0.42 (s, 18 H, CH_3) ppm. $^{13}C\{^1H\}$ NMR (CD_3CN): δ = 154.8 (d, $^1J_{C,F}$ = 241.0 Hz, C_{ortho}), 140.7 (d, $^2J_{H,F}$ = 13.0 Hz, C_{ipso}), 127.3 (C_{ortho}), 126.3 (d, $^3J_{C,F}$ = 7.3 Hz, C_{para}), 125.5 (d, $^4J_{C,F}$ = 3.7 Hz, C_{meta}), 116.9 (d, $^2J_{C,F}$ = 22 Hz, C_{meta}), 52.4 (NCH_2CH_2N), –0.7 (CH_3) ppm. ^{19}F NMR(CD_3CN): δ = –41.06 (m) ppm. $C_{30}H_{42}F_3IN_6Si_3Ti$ (802.72): calcd. C 44.86, H 5.27, N 10.47; found C 44.68, H 5.27, N 10.37. MS (EI): m/z = 675 [M – I]$^+$.

[Ti{N(Ph)SiMe$_2$}$_3$-tacu]I (8): A solution of [Ti{N(Ph)SiMe$_2$}$_3$-tacu] (3.25 g, 5.0 mmol) in toluene at –60 °C was treated with I_2 (0.69 g, 2.7 mmol). The solution was allowed to warm to room temperature and was then stirred for 12 h. The solvent was removed in vacuo and the residue was washed with hexane (3×5 mL) and dried. The complex was obtained as an orange solid in 96% yield (3.72 g). ^1H NMR (CD_2Cl_2, room temp.): δ = 7.14 (t, $^3J_{H,H}$ = 7.5 Hz, 2 H, H_{meta}), 6.91 (m, 4 H, H_{meta}), 6.68 (m, 3 H, H_{para}), 6.49 (d, $^3J_{H,H}$ = 7.5 Hz, 2 H, H_{ortho}), 6.25 (d, $^3J_{H,H}$ = 7.8 Hz, 4 H, H_{ortho}), 3.68, 3.39 (br., 4 H, NCH_2CH_2N), 3.47, 3.30 (m, 8 H, NCH_2CH_2CH_2N), 2.37, 2.05 (br., m, 4 H, NCH$_2$CH_2CH_2N), 0.70 (s, 6 H, CH_3), 0.46 (s, 6 H, CH_3), 0.21 (br. s, 6 H, CH_3) ppm. ^1H NMR (CD_2Cl_2, –40 °C): δ = 7.10 (m, 2 H, H_{meta}), 6.97–6.84 (m, 4 H, H_{meta}), 6.69–6.23 (m, 3 H, H_{para}), 6.51 (d, $^3J_{H,H}$ = 7.8 Hz, 2 H, H_{ortho}), 6.40 (d, $^3J_{H,H}$ = 7.8 Hz, 2 H, H_{ortho}), 6.23 (d, $^3J_{H,H}$ = 8.1 Hz, 2 H, H_{ortho}), 3.70–3.14 (br. m, 12 H, NCH_2), 2.10, 1.89 (br. m, 4 H, NCH$_2$CH_2CH_2N), 0.83 (s, 3 H, CH_3), 0.75 (s, 3 H, CH_3), 0.43 (s, 6 H, CH_3), 0.21 (s, 3 H, CH_3), 0.12 (s, 3 H, CH_3) ppm. ^1H NMR (CD_2Cl_2, –70 °C): δ = 7.08 (m, 2 H, H_{meta}), 6.94 (m, 2 H, H_{meta}), 6.83 (m, 2 H, H_{meta}), 6.67–6.51 (m, 7 H, H_{para}, H_{ortho}), 6.25 (br. d, 2 H, H_{ortho}), 3.70–3.06 (br. m, 12 H, NCH_2), 2.07, 1.76 (br. m, 4 H, NCH$_2$CH_2CH_2N), 0.95 (s, 3 H, CH_3), 0.78 (s, 3 H, CH_3), 0.44

Table 5. Crystal and refinement data for compound **6**.

	6
Empirical formula	$C_{32}H_{49}N_6Si_3Ti$
Formula mass	649.94
Temperature	293(2) K
Wavelength	1.54180 Å
Crystal system	triclinic
Space group	$P\bar{1}$
Unit cell dimensions	a = 10.497(3) Å b = 18.309(6) Å c = 18.355(3) Å
Volume	3481.6(16) Å^3
Z	2 (2 molecules)
Calculated density	1.240 Mg m^{-3}
Absorption coefficient	3.304 mm^{-1}
F(000)	1388
Crystal morphology	prism
Crystal size	0.6×0.3×0.2 mm
Colour	orange
Theta range for data collection	3.25 to 66.93°
Limiting indices	$-12 \le h \le 0$ $-21 \le k \le 21$ $-21 \le l \le 21$
Reflections collected/unique	13100/12362 [R(int) = 0.0721]
Completeness to theta	99.8% (θ = 66.93)
Refinement method	full-matrix least-squares on F^2
Data/restraints/parameters	12362/0/758
Goodness-of-fit on F^2	0.987
Final R indices [$I > 2\sigma(I)$]	$R1$ = 0.0908, $wR2$ = 0.2300
R indices (all data)	$R1$ = 0.1767, $wR2$ = 0.2726
Largest diff. peak and hole	0.625 and –0.551 e Å^{-3}

(s, 3 H, CH_3), 0.38 (s, 3 H, CH_3), 0.21 (s, 3 H, CH_3), 0.09 (s, 3 H, CH_3) ppm. $^{13}C\{^1H\}$ NMR (CD_2Cl_2, room temp.): δ = 159.0, 152.8 (C_{ipso}), 129.6, 128.8, 124.1, 122.9, 119.7, 118.6 (C_{Ph}), 52.6, 50.7, 48.3 (NCH_2), 26.7 (NCH$_2$$CH_2$$CH_2$N), 1.8 ($CH_3$), 1.1 ($CH_3$), 0.0 ($CH_3$) ppm. $C_{32}H_{49}IN_6Si_3Ti$ (776.80): calcd. C 49.48, H 6.36, N 10.82; found C 49.18, H 6.27, N 10.39.

X-ray Experimental Details: X-ray data were collected on a MACH3 Nonius diffractometer equipped with Mo-K_α radiation (λ = 0.71069 Å) and a Turbo CAD4 with a rotating anode and Cu-$K_{\alpha1}$ radiation (in the case of compound **7**), at room temperature. Solution and refinement were performed with SIR97[20] and SHELXL[21] included in the WINGX Version 1.64.03b program package.[22] Compound **5** crystallized in the cubic space group $P2_13$, thus only 1/3 of the molecule is present in the asymmetric unit, as the Ti atom is on a 3-fold rotation axis. Compound **6** crystallized in the triclinic centrosymmetric space group $P\bar{1}$ with two similar molecules in the asymmetric unit. Geometrical data are discussed and presented only for one of the molecules. As for compound **7**, a large residual electron density is present near the iodide atom. Several refinements of a possible disorder of I^- (occupying three possible positions with different occupation factors) did not improve the refinement and several satellite residual peaks were kept. The possibility of a disordered I_3^- ion was also attempted but the I–I distances were not acceptable. All non-H atoms were refined anisotropically, and all hydrogen atoms were inserted in idealized positions riding on the parent C atom. All the details concerning data collection and refinement are presented in Table 4 and Table 5. Figures were drawn with ORTEP3.[23]

CCDC-250633 to -250635 (for **5**–**7**, respectively) contain the supplementary crystallographic data for this paper. These data can be obtained free of charge from The Cambridge Crystallographic Data Centre via www.ccdc.cam.ac.uk/data_request/cif.

Acknowledgments

The authors are thankful to the Fundação para a Ciência e a Tecnologia, Portugal for funding this work (research projects POCTI/QUI/39734/2001 and POCTI/QUI/46206/2002).

[1] J. Costamagna, G. Ferraudi, B. Matsuhiro, M. C. Vallette, J. Canales, M. Villagrán, J. Vargas, M. Aguirre, *Coord. Chem. Rev.* **2000**, *196*, 125–164.
[2] J. P. Danks, N. R. Champness, M. Schröder, *Coord. Chem. Rev.* **1998**, *174*, 417–468.
[3] K. P. Wainwright, *Coord. Chem. Rev.* **1997**, *166*, 35–90.
[4] O. Schlager, K. Wieghardt, B. Nuber, *Inorg. Chem.* **1995**, *34*, 6456–6462.
[5] C. M. Cui, G. R. Giesbrecht, J. A. R. Schmidt, J. Arnold, *Inorg. Chim. Acta* **2003**, *351*, 404–408.
[6] J. A. R. Schmidt, G. R. Giesbrecht, C. M. Cui, J. Arnold, *Chem. Commun.* **2003**, 1025–1033.
[7] C. G. J. Tazelaar, S. Bambirra, D. van Leusen, A. Meetsma, B. Hessen, J. H. Teuben, *Organometallics* **2004**, *23*, 936–939.
[8] S. Bambirra, S. J. Boot, D. van Leusen, A. Meetsma, B. Hessen, *Organometallics* **2004**, *23*, 1891–1898.
[9] A. R. Dias, A. M. Martins, J. R. Ascenso, H. Ferreira, M. T. Duarte, R. T. Henriques, *Inorg. Chem.* **2003**, *42*, 2675–2682.
[10] B. Monteiro, D. Roitershtein, H. Ferreira, J. R. Ascenso, A. M. Martins, Â. Domingos, N. Marques, *Inorg. Chem.* **2003**, *42*, 4223–4231.
[11] G. H. Searle, R. J. Geue, *Aust. J. Chem.* **1984**, *37*, 959–962.
[12] T. J. Atkins, J. E. Richman, W. F. Oettle, *Org. Synth.* **1978**, *58*, 652–654.
[13] O. Schlager, K. Wieghardt, H. Grondey, A. Rufinska, B. Nuber, *Inorg. Chem.* **1995**, *34*, 6440–6448.
[14] B. P. Hay, R. D. Hancock, *Coord. Chem. Rev.* **2001**, *212*, 61–78.
[15] E. L. Hegg, S. H. Mortimore, C. L. Cheung, J. E. Huyett, D. R. Powell, J. N. Burstyn, *Inorg. Chem.* **1999**, *38*, 2961–2968.
[16] J. Langmaier, Z. Samec, V. Varga, M. Horáček, K. Mach, *J. Organomet. Chem.* **1999**, *579*, 348–355.
[17] U. Auerbach, T. Weyhermüller, K. Wieghardt, B. Nuber, E. Bill, C. Burzlaff, A. X. Trautwein, *Inorg. Chem.* **1993**, *32*, 508–519.
[18] S. Back, R. A. Gossage, G. Rheinwald, I. del Rio, H. Lang, G. van Koten, *J. Organomet. Chem.* **1999**, *582*, 126–138.
[19] L. E. Manzer, *Inorg. Synth.* **1982**, *21*, 135–137.
[20] Sir97: A new tool for crystal structure determination and refinement: A. Altomare, M. C. Burla, M. Camalli, G. Gascarano, C. Giacovazzo, A. Guagliardi, A. G. G. Moliterni, G. Polidori, R. Spagna, *J. Appl. Crystallogr.* **1999**, *32*, 115–119.
[21] G. M. Sheldrick, *SHELXL, a program for refining crystal structures*, University of Göttingen, Germany, **1997**.
[22] V1.64.03b: L. J. Farrugia, X. Wing, *J. Appl. Crystallogr.* **1999**, *32*, 837–838.
[23] ORTEP3: L. J. Farrugia, *J. Appl. Crystallogr.* **1997**, *30*, 565–566; based on ORTEP-III, v.1.0.3., by C. K. Johnson and M. N. Burnett.

Received: September 28, 2004

